New Astronomy 93 (2022) 101751

Contents lists available at ScienceDirect

New Astronomy

journal homepage: www.elsevier.com/locate/newast

Study on the variation of orbital period, quasi-periodic oscillations and negative superhumps in V729 Sgr

Qi-Bin Sun [a,b], Sheng-Bang Qian [a,b,c,*], Ai-Jun Dong [a,b,**], Qi-Jun Zhi [a,b], Zhong-Tao Han [c], Wei Liu [c], Xin Chang [d], Chang Liu [a,b], Hong-Bin Xiang [a,b], Xue-Bing Peng [a,b], Bin Zhang [a,b], Xu-Dong Zhang [a,b], Fernández Lajús, E [e]

[a] School of Physics and Electronic Science, Guizhou Normal University, Guiyang 550001, China
[b] Guizhou Provincial Key Laboratory of Radio Astronomy and Data Processing, Guizhou Normal University, Guiyang, 550001, China
[c] Yunnan Observatories, Chinese Academy of Sciences (CAS), Kunming, 650011, China
[d] Department of Physics, Yunnan Normal University, Kunming, 650500, China
[e] Instituto de Astrofísica de La Plata (CCT La plata - CONICET/UNLP), Argentina

ARTICLE INFO

Keywords:
Stars
Binaries
Eclipsing stars
Dwarf novae stars
Evolution stars
Individual
V729 sgr

ABSTRACT

Based on K2 and our observations of V729 Sgr, the study of the variation of orbital period, quasi-periodic oscillations (QPOs) and negative superhumps are presented. Using all available mid-eclipse times during quiescence, we find that V729 Sgr has a cyclic variation of the orbital period, with periods and amplitudes of ∼9.64 years and ∼442.37 s, respectively. Based on the interpret of light travel-time effect, the mass of third body is derived as $M_3 sini' = 0.24(\pm 0.016) M_{\odot}$. When the third body is coplanar with the central body system, the third body may be a low-mass star. Using the Weighted Wavelet Z-transform (WWZ) method, we find for the first time that V729 Sgr has QPOs with the period of ∼1030–3370 s. Using WWZ method, we find that V729 Sgr also has negative superhumps in the first quiescence, indicating that the negative superhumps may be permanent in the quiescence of V729 Sgr.

1. Introduction

Dwarf novae (DN) are a subclass of cataclysmic variable stars (CVs), which belong to semi-detached close binary stars composed of a white dwarf (the primary star) and a late-type star (the secondary star or the donor). The secondary star overfills its Roche lobe, and the white dwarf accretes the material of the secondary star through the inner Lagrange point (L1). The material from the secondary star has angular momentum and cannot immediately fall to the white dwarf to form an accretion disk around the white dwarf. The accretion flow from the secondary star forms a bright collision zone (hot spot) with the edge of the accretion disk (Warner, 1995). DN show that intermittent outburst, the light increases about 2–5 magnitude from a few days to a few weeks, the outburst lasts for several days to dozens of days, and the recurrent time is between a few days and a few years. The disk instability model can explain the mechanism of outbursts (DIM; Lasota, 2001; Hameury, 2020).

The orbital period change can be seen from the observed-minus-calculated (O-C) of mid-eclipse times. Current research shows that orbital cyclic variation widely exist in CVs, such as U Gem (Dai and Qian, 2009), EX Dra (Han et al., 2017c), DV UMa (Han et al., 2017b), OY Car (Han et al., 2015), Z Cha (Dai et al., 2009), SW Sex (Fang et al., 2020), V2051 Oph (Qian et al., 2015) and EM Cyg (Liu et al., 2021). Mechanism of cyclic variation is commonly interpreted as the existence of a solar-type magnetic activity cycle in the secondary star (Applegate, 1992) or the light travel-time effect caused by the existence of the third body (Irwin, 1952).

It is generally accepted that DN have three types of rapid oscillations: DN oscillations (DNOs), long-period DN oscillations (lp-DNOs), and quasi-periodic oscillations (QPOs) (Warner, 2004; Pan and Dai, 2019). The period of QPOs is longer than that of DNOs, ranging from hundreds to thousands of seconds. QPOs widely exist in CVs. Warner (2004) proposed at least three types of QPO after statistical analysis of about 50 CVs. The first one is DNO-related QPOs, which coexists with DNOs and oscillates several hundred seconds. The second is IP-related QPOs, which have an oscillation period of about 1000 s. Its generation is related to the structure of intermediate polars (IPs) (Patterson et al., 2002). Except for DNO-related QPOs and IP-related QPOs, the remaining QPOs are the third (Other QPOs), and there is no

* Corresponding author at: Yunnan Observatories, Chinese Academy of Sciences (CAS), Kunming, 650011, China.
** Corresponding author at: School of Physics and Electronic Science, Guizhou Normal University, Guiyang 550001, China.
E-mail addresses: qsb@ynao.ac.cn (S.-B. Qian), aijdong@gznu.edu.cn (A.-J. Dong).

https://doi.org/10.1016/j.newast.2021.101751
Received 14 October 2021; Received in revised form 26 November 2021; Accepted 6 December 2021
Available online 1 January 2022

relevant theoretical model to describe them (Warner, 2004; Scepi et al., 2021).

There are generally two types of superhumps in CVs, one is the positive superhumps with a period greater than several percentages of orbital period, and the other is the negative superhumps with a period shorter than several percentages of the orbital period. The commonly accepted explanation for the origin of the positive superhumps are caused by the tidal stress of the secondary star on the disk (Vogt, 1982; Osaki, 1985; Wood et al., 2011), and the negative superhumps are caused by the precession of a tilted disk (Bonnet-Bidaud et al., 1985; Patterson, 1999; Harvey et al., 1995).

V729 Sgr was detected as variable star by Gent (1932), then Ferwerda (1934) suggested this star may be an irregular variable, and was classified as a CVs by Cieslinski et al. (1997, 1998). It was classified as a Z Cam-type eclipsing DN by Cieslinski et al. (2000). Ramsay et al. (2017) based on the K2 observation results of V729 Sgr, it is found that V729 Sgr has a rare high outburst frequency of long-period DN, and there are negative superhumps in 5 of 6 quiescence. The research of Han et al. (2017a) shows that V729 Sgr has DNOs of ~25.5 s and ~36.2 s, lpDNOs of ~136 s and ~154 s, and QPOs of ~231–478 s.

This paper studies the variation of orbital period, QPOs, and negative superhumps based on K2 and our observations of V729 Sgr. This paper is structured as follows: Section 2 briefly describes the V729 Sgr data observed by K2, our observations of V729 Sgr, and the calculation of mid-eclipse times and minima. Section 3 analyzes the orbital period changes, the changes in the light minima, and detects QPOs and negative superhumps. Section 4 discusses the quasi-period variation of the orbital period and the QPOs. Section 5 is the summary.

2. Observation and data preparation

2.1. K2 data

Kepler is a space telescope launched in 2009 (Borucki et al., 2010). In 2013, the observation strategy changed due to the failure of two reaction wheels, and the mission was renamed K2 (Howell et al., 2014; Dai et al., 2016). The observation of K2 has long cadence (30 min) mode and short cadence (1 min) mode. K2 observed V729 Sgr in short cadence (1 min) mode during Campaign 9,[1] and the exposure time is the 60 s, and observation wavelengths range from 420 to 910 nm. The observation time is from October 4, 2015 (MJD 57299.74490627) to December 26, 2015 (MJD 57382.3579675), with a total of ~81 days, which provides a lot of data support for our study. We used the data from the Mikulski Archive for Space Telescopes (MAST).[2]

2.2. Followup photometry

We obtained an eclipse curve of V729 Sgr observed by Jorge Sahade Telescope (JST) (see Fig. 1). On October 3, 2021, V729 Sgr was monitored photometrically by using the 2.15 m Jorge sahad telescope (JST) located in Complejo Astronómico El Leoncito (CASLEO), San Juan, Argentina. The integration time is ~5–15 s and no filters were used. The CCD image was measured by using the aperture photometry package of Image Reduction and Analysis Facility (IRAF)[3].

[1] https://keplerscience.arc.nasa.gov/k2-fields.html
[2] https://mast.stsci.edu/
[3] IRAF is a software distributed by the National Optical Astronomical Observatory (NOAO), which aims to reduce astronomical images in the form of a pixel array.

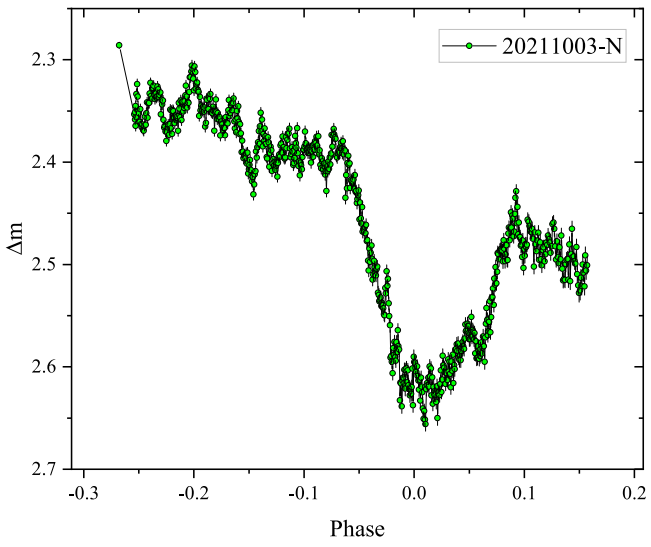

Fig. 1. The light curve of V729 Sgr observed by JST in N-band.

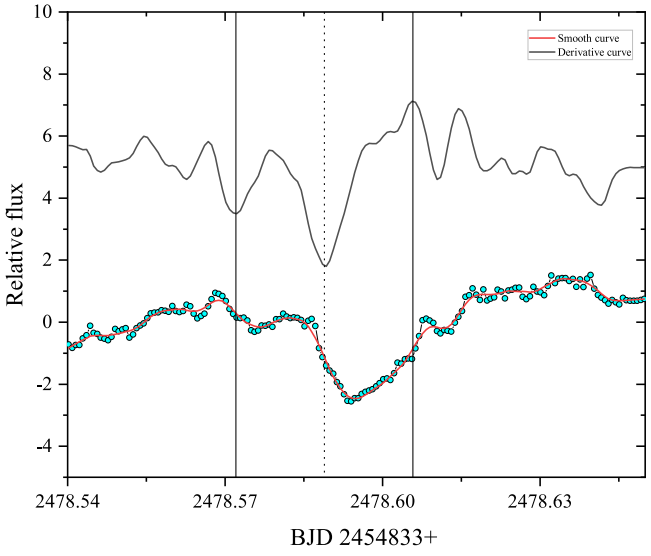

Fig. 2. Example of determining mid-eclipse times of the white dwarf. The two vertical solid lines represent the mid-ingress and mid-egress times of the white dwarf, and the vertical dotted line represents the mid-eclipse times of the white dwarf.

2.3. Calculation of the mid-eclipse times and the minima

The method of obtaining the mid-eclipse times of the white dwarf was described by Wood et al. (1985). We used the same method as them to extract the mid-eclipse times (see Fig. 2). Based on K2 and our data, we obtained 86 mid-eclipse times during quiescence. Combined with historical mid-eclipse times (Cieslinski et al., 2000; Han et al., 2017a), a total of 118 mid-eclipse times are available (see Table 4). We did not use the mid-eclipse times of Ramsay et al. (2017), which was calculated based on the linear plus Gaussian function to calculate the K2 light curves but used the method of Wood et al. (1985) to calculate the mid-eclipse times of white dwarf. In the observation of Cieslinski et al. (2000), except for E = 98 and E = 271, the O-C values of other data are mainly distributed in −0.0016–0.0038 days, while the O-C values of E = 98 and E = 271 are ~0.01 days (~14 minutes; see Table 4). Maybe they are in the outburst, so E = 98 and E = 271 are not used for the study of orbital period changes.

Each eclipse has a minimum brightness, which represents the brightness center of the primary star (including white dwarf, accretion disk,

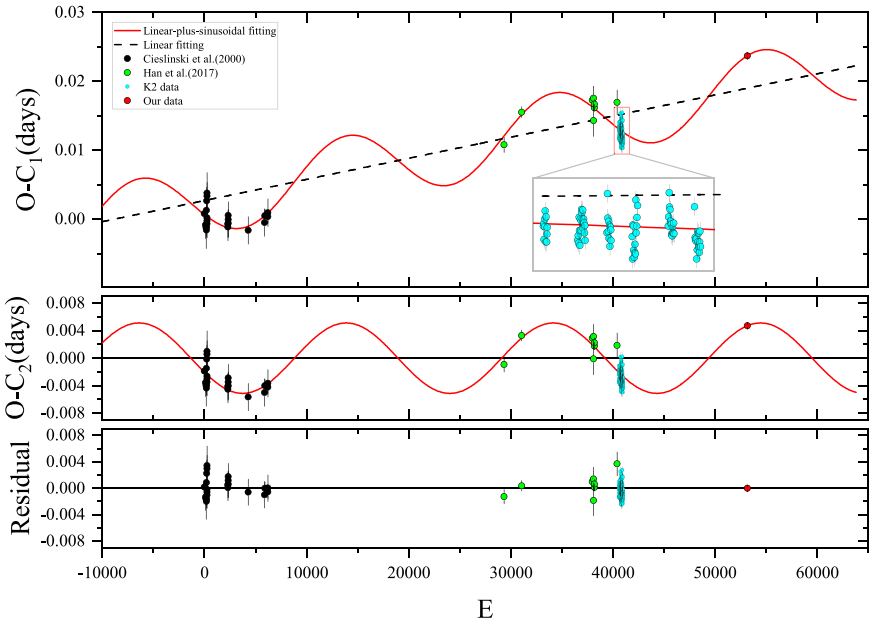

Fig. 3. The O-C diagram of mid-eclipse times in V729 Sgr. Red solid line is the linear-plus-sinusoidal fitting, and the black dashed line is the linear fitting. The middle plate is the O-C diagram without linear trend, and the bottom plate is the residual of linear-plus-sinusoidal fitting.

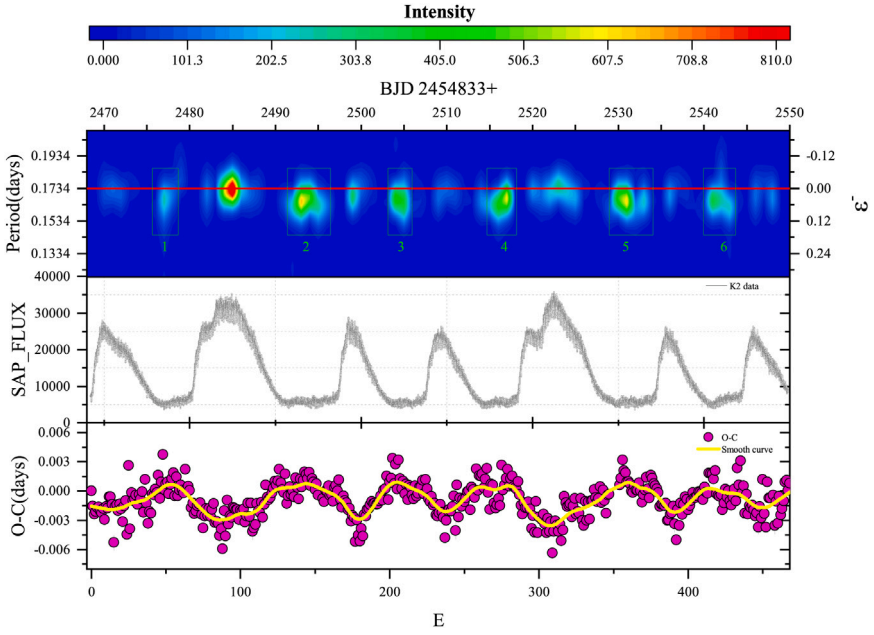

Fig. 4. Two-dimensional power spectra of WWZ, light curve, and O-C diagram of all minima in V729 Sgr. The top plate is the two-dimensional power spectra of WWZ of all K2 data, the middle plate is the light curve, and the bottom plate is the O-C diagram of all minima, and the data is provided by K2. The red line in two-dimensional power spectra is the orbital period of V729 Sgr.

and hot spot), so we use the minima to study the changes in the brightness center of the primary star. We used parabolic fitting to calculate the times of light minima observed by K2 and got 460 minima in total (including quiescence and outburst).

3. Analysis

3.1. Orbital period changes

Using all available mid-eclipse times during quiescence, we study the orbital period changes. The ephemeris of V729 Sgr was derived by Cieslinski et al. (2000):

$$T_{mid-eclipse} = BJD2450269.5794(5) + 0.1734055(5) \times E \quad (1)$$

which was used to calculate the O-C values of V729 Sgr. BJD 2450269.5794(5) is the initial epoch, 0.1734055(5) is the orbital period, and E is the number of circles. We carried out a linear fitting on the O-C values, and the results show that the linear fitting cannot fully explain the change (see Fig. 3). We tried to fit it with linear-plus-sinusoidal fitting (see Fig. 3):

$$O - C = \triangle T_0 + \triangle P_0 \times E + K sin(\omega \times E + \varphi) \quad (2)$$

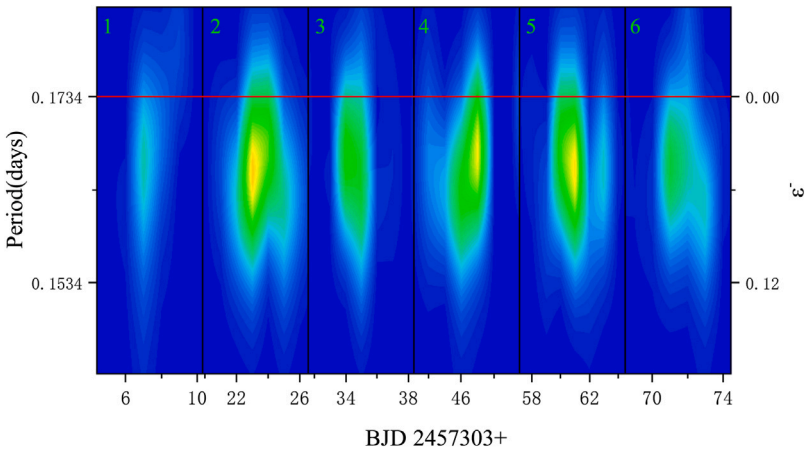

Fig. 5. An enlarged view of the negative superhumps during quiescence. The number in the upper left corner corresponds to Fig. 4.

Table 1
Parameters based on O-C analysis.

Parameters	Values
Revised epoch, $\triangle T_0$ (days)	0.0027(±0.00056)
Revised period, $\triangle P_0$ (days)	$3.07(\pm0.012)\times10^{-7}$
The semi-amplitude, K (days)	0.0051(±0.00021)
Orbital period, $P_3=\frac{2\pi}{\omega}\times P$ (yr)	9.64(±0.013)
Orbital phase, φ (deg)	563.69(±10.41)

$\triangle T_0$ and $\triangle P_0$ are corrections for the epoch and orbital period, and K is the amplitude of cyclic variation. To describe the goodness-of-fit of the two models, the corresponding χ^2 were calculated. It is found that the linear fitting $\chi^2=25.40$, while the linear-plus-sinusoidal fitting $\chi^2=2.18$. Therefore, the use of linear-plus-sinusoidal fitting will significantly advance the fitting (see Fig. 3). According to the fitting results (see Table 1), the orbital period of V729 Sgr may have a cyclic variation with a period and amplitude of ∼9.64 years and ∼442.37 s, respectively.

3.2. Changes in the light minima

Based on the 460 minima of V729 Sgr observed by K2, we study the changes in the light minima. Using a new epoch:

$$T_{minima}=BJD2457301.5397(2)+0.1734058(5)\times E \quad (3)$$

we calculated the O-C value. $BJD2457301.5397(2)$ is our calculated initial time of light minima, and 0.1734058(5) is our corrected orbital period. By comparing the O-C diagram with the light curve, it can be found that the O-C diagram and the light curve have an opposite trend (see Fig. 4). The O-C decreases with the rise of the outburst and increases with the decline of the outburst in an outburst cycle, suggesting that the times of light minima at the time of outburst are earlier than quiescence.

Ramsay et al. (2017) have found that the times of light minima of V729 Sgr during outburst is earlier than quiescence. This phenomenon has also been found in other DN, such as V447 Lyr (Ramsay et al., 2012) and KIS J192748.53+444724.5 (Scaringi et al., 2013). They gave a reasonable explanation that the light fraction of the hot spots in quiescence is significant, and the light fraction of the hot spot decreases when it bursts, so the minima are earlier than that in quiescence. The difference of brightness fraction of hot spot in different states leads to the change of minima, which can be well revealed by the O-C method.

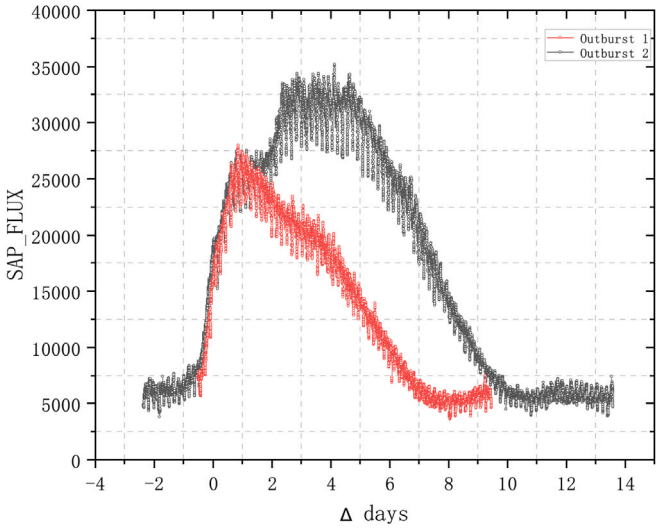

Fig. 6. Two types of outbursts of V729 Sgr. We have folded Outburst 1 and Outburst 2, representing two typical outbursts of V729 Sgr. We use the fastest rising point as the time zero (using the method of deriving the light curve).

3.3. The detection of QPOs

Fig. 4 shows that there are two types of outbursts of V729 Sgr, which are a short outburst with a duration of ∼8 days and a long outburst with a duration of ∼12 days. In addition to the duration of the outburst, another obvious feature of the long outburst is the appearance of a plateau when it rises to maximum brightness (See Ramsay et al. (2017) and Fig. 6). We selected Outburst 1 and Outburst 2 of two different types of outbursts to detect QPOs. We divided outburst 1 into outburst rising (R), maximum (M), decline (D), and quiescence (Q) stages, while outburst 2 we added the middle (Mid) stage (See Fig. 7). Since there is less eclipse during the rise of the outburst, we chose 3 out-of-eclipse curves (∼0.49 days) to detect QPOs, and we also selected 3 out-of-eclipse curves uniformly in other stages. We chose the intermediate stage in the decline of the outburst. The light curves of V729 Sgr in the quiescence are asymmetrical, and the intermediate stage is difficult to confirm, so we chose the minimum brightness stage in quiescence.

It is known that the orbital period, the outburst, and the negative superhumps will affect the detection of QPOs, so we first removed the eclipse part to get the out-of-eclipse curves. Then, locally weighted regression (LOWESS) (Cleveland, 1979) with a smoothing span of 0.1

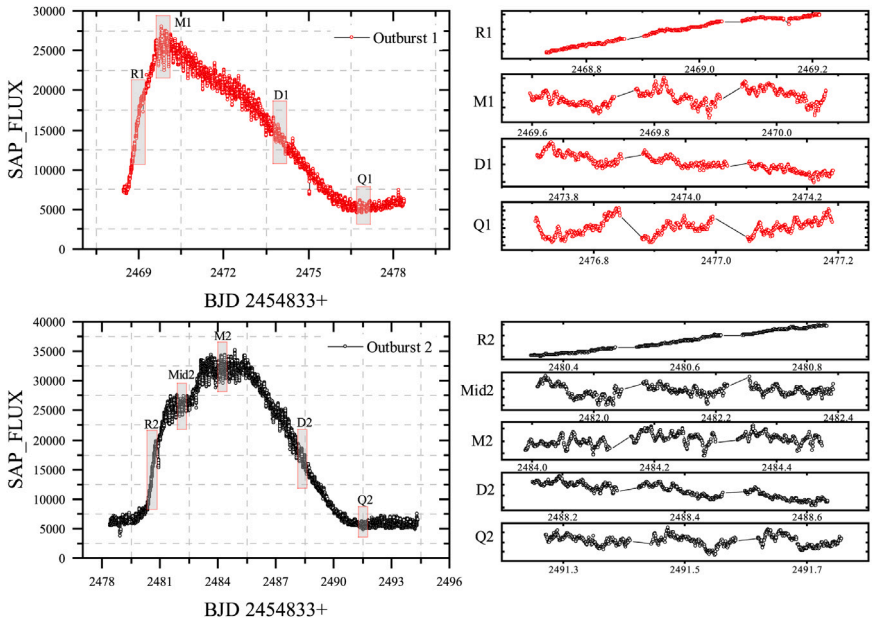

Fig. 7. The out-of-eclipse curves of Outburst 1 and Outburst 2. The selected part of the rectangular box corresponds to the second column of Table 2. The data gap is the removed eclipse.

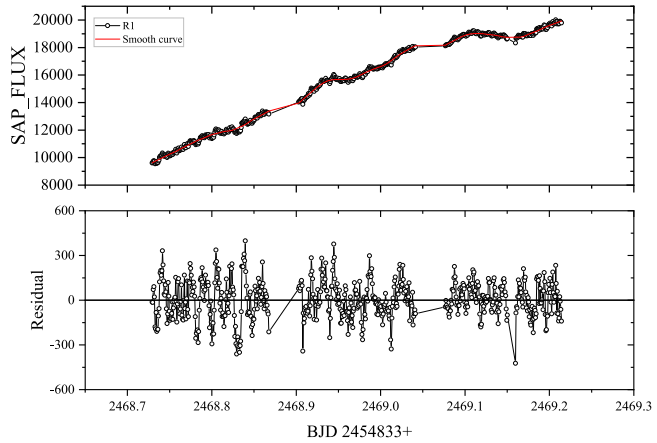

Fig. 8. Example of removing the trend of outburst and the effect of negative superhumps from the light curve. The red curve is the smooth curve, and the lower plate is the light curve minus the outburst trend. The data gap is the removed eclipse.

was used to smooth the light curves we selected. We subtracted the smooth curve from the original light curves to obtain the light curves with the trend of outburst and the effect of negative superhumps removed (See Fig. 8). Finally, the QPOs was detected using the Weighted Wavelet Z-transform (WWZ) (Foster, 1996). We have made statistics on the peaks of two-dimensional power spectra of WWZ (See Table 2, Fig. 9). The uncertainty is based on the half-width at half maximum (HWHM) of Gaussian fitting centered on the power. It is found that a single frequency cannot sufficiently define the light curve of V729 Sgr and has QPOs with the frequency of 25.63–83.84 days^{-1} (~1030–3370 s).

3.4. The detection of negative superhumps

We used WWZ to detect the negative superhumps, and it could obtain the distribution of the signal in the time and frequency domains simultaneously. After using WWZ for all photometric data from K2, the two-dimensional power spectra of WWZ were obtained (see Fig. 4 top plate). It can be found that there are periodic signals shorter than the orbital period in quiescence. Ramsay et al. (2017) found that there were no negative superhumps in the first quiescence, and no superhumps were found in the outburst using LSP and Discrete Fourier Transforms (DFT) methods. By comparing the light curves with the two-dimensional power spectra of WWZ, we found negative superhumps in the first quiescence, but the periodic signal intensity was relatively weak (See the first green rectangle in Figs. 4 and 5). The right axis of the two-dimensional power spectra of WWZ was processed as the negative superhumps excess $\epsilon^- = (P_{orb} - P_{sh})/P_{orb}$. Through the two-dimensional power spectra of WWZ, it can be found that the negative superhumps excess $\epsilon^- \sim 0.05$, which is consistent with the conclusion of Ramsay et al. (2017).

4. Discussion

4.1. Quasi-period variation of orbital period

We found that the orbital period of V729 Sgr has quasi-period variation, with a period of ~9.64 years and an amplitude of ~442.37 s. As for the causes of the cyclic variation of the orbital period, the Applegate's mechanism and the light travel-times effect will be discussed, respectively. In the Applegate's mechanism, due to the magnetic activity of the secondary star, there is an angular momentum transfer between the inner core and outer shells of the secondary star, resulting in the change of the gravitational quadrupole moment (Applegate, 1992). Based on the formula:

$$\frac{\triangle P}{P} = 2\pi \frac{K}{P_3} \tag{4}$$

and parameters estimated by Cieslinski et al. (2000): $M_1 = 0.75 M_\odot$, $M_2 = 0.39 M_\odot$, $R_2 = 0.46 R_\odot$, the binary interval $a = 1.37 R_\odot$ obtained by using Kepler's third law. The fractional period change was calculated as $\triangle P/P = 9.14 \times 10^{-6}$. Based on the calculation formula of gravitational quadrupole moment change:

$$\frac{\triangle P}{P} = -9(\frac{R_2}{a})^2 \frac{\triangle Q}{M_2 R_2^2} \tag{5}$$

the quadrupole moment of the secondary star was calculated as $\triangle Q = 7.21 \times 10^{48}$ g cm^2. Using the same method as Brinkworth et al. (2006),

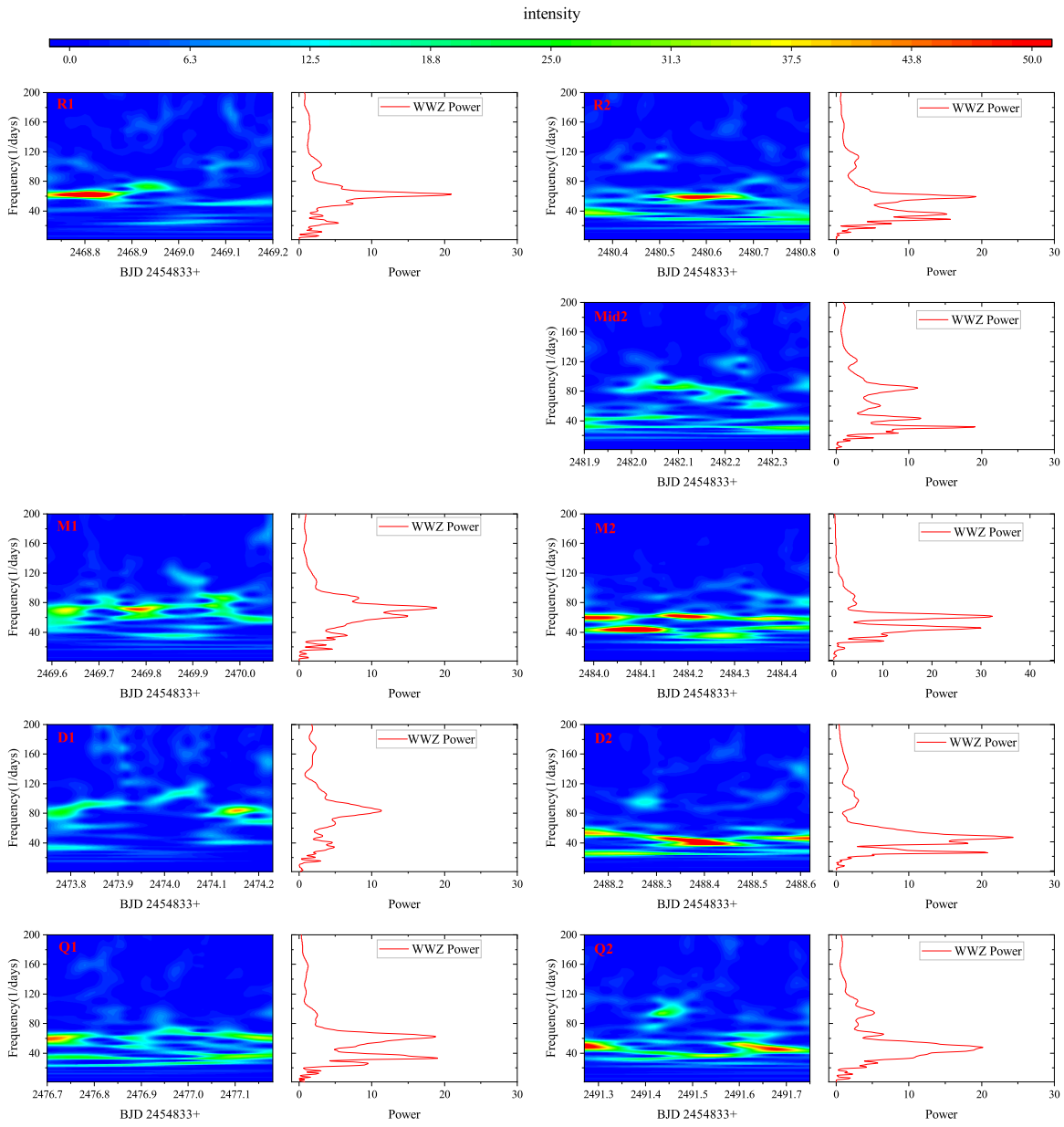

Fig. 9. Two-dimensional power spectrum of WWZ corresponding to Outburst 1 and Outburst 2. The time ranges of R1, M1, D1, Q1, R2, Mid2, M2, D2 and Q2 correspond to Table 2.

the energy of magnetic activity required to cause the cyclic variation of V729 Sgr was calculated (see Fig. 10). The temperature of $T_{eff} \sim 3431$ K for the secondary star was used the luminosity $L_2 = 4\pi R_2^2 \sigma T_{eff}^4$ to calculate, and the total radiation energy of the secondary star is $E \sim 3.15 \times 10^{40}$ erg in 9.64 years. When $M_{shell} = 0.057 M_{\odot}$, the minimum energy needed for cyclic variation is $\triangle E_{min} \sim 1.07 \times 10^{42}$ erg. Therefore, the total energy radiated by the secondary star in 9.64 years cannot provide the energy required for magnetic activity. So, it is tough to explain the cyclic variation of V729 Sgr by the magnetic activity of secondary stars. Another possible mechanism is the light travel-times effect of the third body. According to the formula:

$$f(m) = \frac{4\pi^2}{GP_3^2} \times (a_{12} sini')^3 = \frac{(M_3 sini')^3}{(M_1 + M_2 + M_3)^2} \tag{6}$$

In the formula G is the gravitational constant, P_3 is orbital period of the third body and i' is the orbital inclination. $a_{12} sini'$ can be determined by:

$$a_{12} sini' = K \times c \tag{7}$$

K is the amplitude of the cyclic variation of orbital period, and c is the speed of light. Using Eqs. (6) and (7), the mass function and the mass of the third body can be derived. The calculation results are shown in Table 3. The mass of third body was derived as $M_3 sini' = 0.24(\pm 0.016) M_{\odot}$. Assuming that the third body is coplanar with the central body system($i' = 90°$), it can be obtained that the mass of the third body is $M_3 = 0.24(\pm 0.016) M_{\odot}$, which may be a low mass star. The analysis shows that the light travel-times effect may cause the cyclic variation of V729 Sgr. However, due to the lack of observation data, our research needs further observation to verify.

4.2. The QPOs

We found that V729 Sgr has QPOs with the period of ~1030–3370 s. It is found that a single period cannot describe the light curve of V729 Sgr, and QPOs are distributed in a range (See Table 2). Similarly, there are similar situations in other CVs, such as TT Ari (900–1600 s) (Patterson et al., 2002; Tremko et al., 1996), EC0528-58 (900–1560 s)

Table 2
The frequency and period of peaks in WWZ power.

Name	Stages[a]	Start time[b] d	End time[b] d	Frequency 1/d	Period s
Outburst1	Rise (R1)	2468.7294	2469.2143	62.03(±0.15)	1392.85(±3.44)
	Maximum (M1)	2469.5970	2470.0813	61.05(±0.73)	1415.35(±16.97)
				73.49(±0.44)	1175.72(±6.98)
	Decline (D1)	2473.7584	2474.2433	83.83(±0.28)	1030.60(±3.49)
	Quiescence (Q1)	2476.7061	2477.1910	34.16(±0.30)	2529.27(±22.21)
				60.84(±0.25)	1420.19(±5.93)
Outburst2	Rise (R2)	2480.3478	2480.8327	28.52(±0.13)	3029.08(±13.83)
				34.70(±0.33)	2489.69(±23.38)
				58.58(±0.16)	1474.89(±4.12)
	Middle (Mid2)	2481.9088	2482.3930	31.24(±0.13)	2765.35(±11.68)
				43.02(±0.24)	2008.31(±11.39)
				83.84(±0.35)	1030.54(±4.30)
	Maximum (M2)	2483.9894	2484.4744	43.39(±0.14)	1991.10(±6.65)
				60.02(±0.10)	1439.52(±2.51)
	Decline (D2)	2488.1507	2488.6343	25.63(±0.11)	3370.42(±10.29)
				37.50(±0.17)	2303.72(±11.39)
				45.82(±0.22)	1885.52(±9.24)
	Quiescence (Q2)	2491.2720	2491.7570	45.58(±0.19)	1895.59(±7.90)

[a]Represents different stages of the light curves.
[b]The start time (BJD 2454833+) and end time (BJD 2454833+) of the selected out-of-eclipse curve, respectively.

Table 3
The parameters for the third body orbit of V729 Sgr.

Parameters	Values
Eccentricity, e	0.0
The semi-amplitude, K (days)	0.0051(±0.00021)
Orbital period, $P_3 = \frac{2\pi}{\omega} \times P$ (yr)	9.64(±0.013)
Projected semi-major axis, $a_{12}sini'(AU)$	0.88(±0.049)
Mass function, $f(m_3)(M_\odot)$,	0.0075(±0.00052)
Mass of the third body, $M_3 sini'(M_\odot)$	0.24(±0.016)
Orbital separation$(i' = 90°), a_3(AU)$	4.14(±0.52)

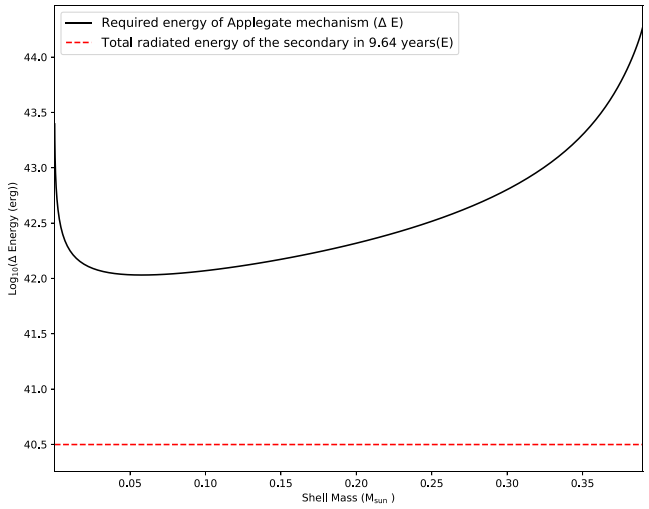

Fig. 10. Energy required to produce the cyclic oscillation in the O-C diagrams using Applegate's mechanism (solid line). The dashed line represents the total energy that radiates from the secondary in 9.64 years.

(Chen et al., 2001), SS Aur (1200–1800 s) (Tovmasian, 1987), V842 Cen (750–1300 s) (Woudt and Warner, 2003), KR Aur (400–900 s) (Kato et al., 2002), SW UMa (280–370 s) (Semeniuk et al., 1997), HX Peg (800–1900 s) (Warner et al., 2003) and VW Hyi (400–600 s) (Warner et al., 2003; Woudt and Warner, 2002; Warner and Woudt, 2002). The QPOs of V729 Sgr are obtained based on the data of ~81 day from K2, and the QPOs detection is more comprehensive. If the observation time is too short, only a few single frequencies or periods may be detected, such as the single out-of-eclipse curve in this paper. Therefore, the detection of QPOs can be fully understood based on long-term observation.

There are several different explanations for the origin of QPOs, such as the internal oscillation of the accretion disk, the reprocessing of light by orbiting blobs (Patterson, 1979), the radial oscillation of accretion disk (Okuda et al., 1992), the interruption and reprocessing of traveling waves in the inner edge of accretion disk (Lubow and Pringle, 1993), and the influence of the magnetic field of the white dwarf star on the accretion disk (Paczyński, 1978). There is a consensus that QPOs widely exist cataclysmic variables with high mass transfer rates, such as nova-like variables and DN in outburst. Another consensus is that QPOs are closely related to accretion disks.

5. Conclusions

In this paper, we used the data of V729 Sgr observed by K2 from October 4, 2015, to December 26, 2015, and the data observed by us on October 3, 2021, to study the variation of orbital period, QPOs, and negative superhumps.

Based on the available mid-eclipse times during quiescence, we conducted O-C analysis and found that V729 Sgr has a cyclic variation of the orbital period with periods and amplitudes of ~9.64 years and ~442.37 s, respectively. The total energy radiated by the secondary star of V729 Sgr in 9.64 years cannot provide the energy required for magnetic activity. The cyclic variation of the orbital period may be caused by the light travel-time effect caused by the existence of the third body. Based on the explanation of light travel-times effect, the mass of third body is derived as $M_3 sini' = 0.24(\pm0.016)M_\odot$. When the third body is coplanar with the central body system, it can be obtained that the mass of the third body is $M_3 = 0.24(\pm0.016)M_\odot$, the third body may be a low mass star.

Using the WWZ method, we found for the first time that V729 Sgr has QPOs with the period of ~1030–3370 s. The QPOs of V729 Sgr cannot be described by several single frequencies or cycles but by a range.

Based on the WWZ method, we found that V729 Sgr has negative superhumps in quiescence. Different from the research of Ramsay et al. (2017), there are still negative superhumps in the first quiescence, but the intensity is relatively weak, which proves that the negative superhumps are permanent in the quiescence of V729 Sgr.

Table 4
The 118 available mid-eclipse times of V729 Sgr for studying the changes of orbital period.

Time (MBJD)	E	O-C (d)	Errors (d)	Ref	Time (MBJD)	E	O-C (d)	Errors (d)	Ref
50269.0802	0	0.0008	0.0005	1	57327.0423	40702	0.0123	0.0007	3
50286.063*	98	−0.0104	0.002	1	57327.2163	40703	0.0129	0.0007	3
50286.246	99	−0.0008	0.002	1	57327.3886	40704	0.0117	0.0007	3
50299.251	174	−0.0013	0.003	1	57336.5797	40757	0.0123	0.0007	3
50301.161	185	0.0013	0.001	1	57336.7561	40758	0.0154	0.0007	3
50302.197	191	−0.0012	0.001	1	57336.9276	40759	0.0135	0.0007	3
50303.239	197	−0.0016	0.001	1	57337.1000	40760	0.0124	0.0007	3
50309.139	231	0.0026	0.002	1	57337.2742	40761	0.0132	0.0007	3
50311.044	242	0.0002	0.002	1	57337.4463	40762	0.0119	0.0007	3
50311.221	243	0.0038	0.003	1	57337.6207	40763	0.0129	0.0007	3
50312.084	248	−0.0003	0.001	1	57337.7925	40764	0.0113	0.0007	3
50312.261	249	0.0033	0.002	1	57337.9673	40765	0.0128	0.0007	3
50313.124	254	−0.0007	0.002	1	57338.1405	40766	0.0126	0.0007	3
50316.061*	271	−0.0116	0.002	1	57338.3131	40767	0.0117	0.0007	3
50668.085	2301	−0.0007	0.002	1	57347.1571	40818	0.0120	0.0007	3
50668.258	2302	−0.0011	0.002	1	57347.3288	40819	0.0103	0.0007	3
50670.166	2313	−0.0006	0.002	1	57347.5048	40820	0.0129	0.0007	3
50672.074	2324	−0.0001	0.001	1	57347.6781	40821	0.0128	0.0007	3
50672.248	2325	0.0005	0.002	1	57347.8497	40822	0.0110	0.0007	3
51012.294	4286	−0.0016	0.002	1	57348.0225	40823	0.0104	0.0007	3
51292.345	5901	−0.0005	0.002	1	57348.1963	40824	0.0108	0.0007	3
51293.213	5906	0.0005	0.001	1	57348.3704	40825	0.0114	0.0007	3
51347.142	6217	0.0004	0.001	1	57348.5430	40826	0.0107	0.0007	3
51348.183	6223	0.0009	0.002	1	57348.7206	40827	0.0149	0.0007	3
55354.3799	29326	0.0108	0.0011	2	57348.8915	40828	0.0123	0.0007	3
55656.2836	31067	0.0155	0.0008	2	57349.0654	40829	0.0128	0.0007	3
56858.1588	37998	0.0172	0.0005	2	57349.2394	40830	0.0135	0.0007	3
56874.2858	38091	0.0175	0.0018	2	57349.4138	40831	0.0144	0.0007	3
56875.1496	38096	0.0143	0.0023	2	57362.4176	40906	0.0129	0.0007	3
56889.1973	38177	0.0161	0.0001	2	57362.5917	40907	0.0136	0.0007	3
56892.1457	38194	0.0167	0.0007	2	57362.7670	40908	0.0154	0.0007	3
57274.1583	40397	0.0169	0.0006	2	57362.9393	40909	0.0143	0.0007	3
57309.7023	40602	0.0128	0.0007	3	57363.1125	40910	0.0141	0.0007	3
57309.8759	40603	0.0130	0.0007	3	57363.2849	40911	0.0132	0.0007	3
57310.0481	40604	0.0118	0.0007	3	57363.4584	40912	0.0132	0.0007	3
57310.2225	40605	0.0128	0.0007	3	57363.6316	40913	0.0130	0.0007	3
57310.3965	40606	0.0134	0.0007	3	57363.8042	40914	0.0122	0.0007	3
57310.5705	40607	0.0140	0.0007	3	57363.9775	40915	0.0121	0.0007	3
57310.7415	40608	0.0116	0.0007	3	57364.1516	40916	0.0128	0.0007	3
57310.9169	40609	0.0136	0.0007	3	57364.3246	40917	0.0123	0.0007	3
57311.0883	40610	0.0116	0.0007	3	57364.4979	40918	0.0123	0.0007	3
57311.2624	40611	0.0122	0.0007	3	57364.6721	40919	0.0131	0.0007	3
57311.4363	40612	0.0127	0.0007	3	57364.8447	40920	0.0123	0.0007	3
57324.2673	40686	0.0118	0.0007	3	57373.5170	40970	0.0143	0.0007	3
57324.4411	40687	0.0121	0.0007	3	57373.6881	40971	0.0120	0.0007	3
57324.6139	40688	0.0115	0.0007	3	57373.8613	40972	0.0118	0.0007	3
57324.7893	40689	0.0135	0.0007	3	57374.0346	40973	0.0117	0.0007	3
57324.9617	40690	0.0125	0.0007	3	57374.2082	40974	0.0119	0.0007	3
57325.1339	40691	0.0114	0.0007	3	57374.3800	40975	0.0103	0.0007	3
57325.3094	40692	0.0134	0.0007	3	57374.5541	40976	0.0110	0.0007	3
57325.4819	40693	0.0125	0.0007	3	57374.7290	40977	0.0124	0.0007	3
57325.6560	40694	0.0132	0.0007	3	57374.9016	40978	0.0116	0.0007	3
57325.8303	40695	0.0141	0.0007	3	57375.0757	40979	0.0123	0.0007	3
57326.0035	40696	0.0139	0.0007	3	57375.2480	40980	0.0112	0.0007	3
57326.1764	40697	0.0134	0.0007	3	57375.4210	40981	0.0108	0.0007	3
57326.3505	40698	0.0141	0.0007	3	57375.5952	40982	0.0116	0.0007	3
57326.5225	40699	0.0127	0.0007	3	57375.7694	40983	0.0125	0.0007	3
57326.6966	40700	0.0134	0.0007	3	57375.9416	40984	0.0113	0.0007	3
57326.8697	40701	0.0131	0.0007	3	59490.1139	53176	0.0237	0.0002	4

Reference: 1. Cieslinski et al. (2000); 2. Han et al. (2017a); 3. Data from K2; 4. Our data. *. E = 98 and E = 271 are not used in the study of orbital period changes. See Section 2 for detailed explanation.

CRediT authorship contribution statement

Qi-Bin Sun: Conceptualization, Methodology, Software, Writing – original draft. **Sheng-Bang Qian:** Conceptualization, Data curation, Project administration, Funding acquisition. **Ai-Jun Dong:** Supervision, Visualization, Investigation, Funding acquisition. **Qi-Jun Zhi:** Resources. **Zhong-Tao Han:** Investigation, Writing – review & editing. **Wei Liu:** Software. **Xin Chang:** Software, Visualization. **Chang Liu:** Investigation. **Hong-Bin Xiang:** Visualization. **Xue-Bing Peng:** Resources. **Bin Zhang:** Writing - review & editing. **Xu-Dong Zhang:** Formal analysis. **Fernández Lajús E:** Data curation.

Declaration of competing interest

The authors declare the following financial interests/personal relationships which may be considered as potential competing interests: Sheng-Bang Qian and Ai-Jun Dong reports financial support was provided by National Natural Science Foundation of China. Ai-Jun Dong

reports financial support was provided by The National Key R&D Program of China and The Science and Technology Foundation of Guizhou province.

Acknowledgments

This work was supported by the National Natural Science Foundation of China (Nos. 11933008, U1831120, U1731238), the Science and Technology Foundation of Guizhou province (Nos. (2019)1241, KY(2020)003), and the National Key R&D Program of China (Nos. 2018YFA0404602). The mid-eclipse times of Han et al. (2017) were provided by them through private communication. This work has made use of the data collected by the K2 mission, which is publicly available at the Mikulski Archive for Space Telescopes (MAST).

References

Applegate, J.H., 1992. A mechanism for orbital period modulation in close binaries. Astrophys. J. 385, 621–629. http://dx.doi.org/10.1086/170967.

Bonnet-Bidaud, J., Motch, C., Mouchet, M., 1985. The continuum varibility of the puzzling X-ray three-period cataclysmic variable 2a0526-328 (TV Col). Astron. Astrophys. 143, 313–320.

Borucki, W.J., Koch, D., Basri, G., Batalha, N., Brown, T., Caldwell, D., Caldwell, J., Christensen-Dalsgaard, J., Cochran, W.D., DeVore, E., et al., 2010. Kepler planet-detection mission: introduction and first results. Science 327 (5968), 977–980.

Brinkworth, C., Marsh, T., Dhillon, V., Knigge, C., 2006. Detection of a period decrease in NN ser with ULTRACAM: evidence for strong magnetic braking or an unseen companion. Mon. Not. R. Astron. Soc. 365 (1), 287–295. http://dx.doi.org/10.1111/j.1365-2966.2005.09718.x.

Chen, A., O'Donoghue, D., Stobie, R., Kilkenny, D., Warner, B., 2001. Cataclysmic variables in the Edinburgh–Cape blue object survey. Mon. Not. R. Astron. Soc. 325 (1), 89–110. http://dx.doi.org/10.1046/j.1365-8711.2001.04322.x.

Cieslinski, D., Jablonski, F., Steiner, J., 1997. Southern and equatorial irregular variables-I. Photoelectric photometry. Astron. Astrophys. Suppl. Ser. 124 (1), 55–56. http://dx.doi.org/10.1051/aas:1997353.

Cieslinski, D., Steiner, J., Jablonski, F., 1998. Southern and equatorial irregular variables-II. Optical spectroscopy. Astron. Astrophys. Suppl. Ser. 131 (1), 119–135. http://dx.doi.org/10.1051/aas:1998424.

Cieslinski, D., Steiner, J., Pereira, P., Pereira, M., 2000. The orbital period of the eclipsing dwarf nova V729 sagittarii. Publ. Astron. Soc. Pac. 112 (769), 349. http://dx.doi.org/10.1086/316540.

Cleveland, W.S., 1979. Robust locally weighted regression and smoothing scatterplots. J. Amer. Statist. Assoc. 74 (368), 829–836.

Dai, Z., Qian, S., 2009. Orbital period analysis of eclipsing dwarf novae: U Geminorum. Astrophys. Space Sci. 321 (2), 91–100. http://dx.doi.org/10.1007/s10509-009-9982-0.

Dai, Z., Qian, S., Lajús, E.F., 2009. Evidence of a brown dwarf in the eclipsing dwarf nova Z Chamaeleonis. Astrophys. J. 703 (1), 109. http://dx.doi.org/10.1088/0004-637X/703/1/109.

Dai, Z., Szkody, P., Garnavich, P.M., Kennedy, M., 2016. Cataclysmic variables observed during K2 campaigns 0 and 1. Astron. J. 152 (1), 5. http://dx.doi.org/10.3847/0004-6256/152/1/5.

Fang, X., Qian, S., Han, Z., Wang, Q., 2020. Long-term period changes and brightness variations for the deeply eclipsing cataclysmic variable SW sex. Astrophys. J. 901 (2), 113. http://dx.doi.org/10.3847/1538-4357/abb1b9.

Ferwerda, J.G., 1934. Two new faint irregular variable stars. Bull. Astron. Inst. Neth. 7, 166.

Foster, G., 1996. Wavelets for period analysis of unevenly sampled time series. Astron. J. 112, 1709–1729. http://dx.doi.org/10.1086/118137.

Gent, H.v., 1932. Provisional ephemerides of 63 new and 3 known variable stars in or near the constellation corona australis (Errata: 6 V). Bull. Astron. Inst. Neth. 6, 163.

Hameury, J.-M., 2020. A review of the disc instability model for dwarf novae, soft X-ray transients and related objects. Adv. Space Res. 66 (5), 1004–1024. http://dx.doi.org/10.1016/j.asr.2019.10.022.

Han, Z.-T., Qian, S.-B., Fernández-Lajús, E., Voloshina, I., Zhu, L.-Y., 2017a. Long-term photometric behavior of the eclipsing cataclysmic variable V729 sagittarii. Publ. Astron. Soc. Japan 69 (3), http://dx.doi.org/10.1093/pasj/psx030.

Han, Z.-T., Qian, S.-B., Irina, V., Zhu, L.-Y., 2017b. Cyclic period oscillation of the eclipsing dwarf nova DV UMa. Astrophys. J. 153 (5), 238. http://dx.doi.org/10.3847/1538-3881/aa6c2a.

Han, Z.-T., Qian, S.-B., Lajús, E.F., Liao, W.-P., Zhang, J., 2015. An orbital period analysis of the dwarf novae OY carinae. New Astron. 34, 1–5. http://dx.doi.org/10.1016/j.newast.2014.04.011.

Han, Z.-t., Qian, S.-b., Voloshina, I., Zhu, L.-Y., 2017c. Double cyclic variations in orbital period of the eclipsing cataclysmic variable EX Dra. Astrophys. Space Sci. 362 (6), 1–7. http://dx.doi.org/10.1007/s10509-017-3091-2.

Harvey, D., Skillman, D.R., Patterson, J., Ringwald, F., 1995. Superhumps in cataclysmic binaries. V. V503 cygni. Publ. Astron. Soc. Pac. 107 (712), 551. http://dx.doi.org/10.1086/133591.

Howell, S.B., Sobeck, C., Haas, M., Still, M., Barclay, T., Mullally, F., Troeltzsch, J., Aigrain, S., Bryson, S.T., Caldwell, D., et al., 2014. The K2 mission: characterization and early results. Publ. Astron. Soc. Pac. 126 (938), 398.

Irwin, J.B., 1952. The determination of a light-time orbit. Astrophys. J. 116, 211. http://dx.doi.org/10.1086/145604.

Kato, T., Ishioka, R., Uemura, M., 2002. Photometric study of KR aurigae during the high state in 2001. Publ. Astron. Soc. Japan 54 (6), 1033–1039. http://dx.doi.org/10.1093/pasj/54.6.1033.

Lasota, J.-P., 2001. The disc instability model of dwarf novae and low-mass X-ray binary transients. New Astron. Rev. 45 (7), 449–508. http://dx.doi.org/10.1016/S1387-6473(01)00112-9.

Liu, W., Qian, S.-B., Zhi, Q.-J., Han, Z.-T., Wang, Q.-S., Dong, A.-J., 2021. Quasi-periodic oscillations and long-term orbital period variation of the eclipsing dwarf nova EM Cyg. Mon. Not. R. Astron. Soc. 505 (1), 677–683. http://dx.doi.org/10.1093/mnras/stab1298.

Lubow, S., Pringle, J., 1993. Wave propagation in accretion disks-axisymmetric case. Astrophys. J. 409, 360–371. http://dx.doi.org/10.1086/172669.

Okuda, T., Ono, K., Tabata, M., Mineshige, S., 1992. Disc oscillation model for quasi-periodic light variations in cataclysmic variables. Mon. Not. R. Astron. Soc. 254 (3), 427–434. http://dx.doi.org/10.1093/mnras/254.3.427.

Osaki, Y., 1985. Irradiation-induced mass-overflow instability as a possible cause of superoutbursts in SU UMa stars. Astron. Astrophys. 144, 369–380.

Paczyński, B., 1978. Phenomenological model of U geminorum. In: Nonstationary Evolution of Close Binaries. p. 89.

Pan, Dai, 2019. Investigations on the observations of three types of periodic oscillations in cataclysmic variables. Acta Astron. Sin. 60 (4), 103–119. http://dx.doi.org/10.1086/118137.

Patterson, J., 1979. Rapid oscillations in cataclysmic variables. III - an oblique rotator in an AE aquarii. Astrophys. J. 234 (3), 978–992. http://dx.doi.org/10.1086/157582.

Patterson, J., 1999. Permanent superhumps in cataclysmic variables. Front. Sci. Ser. 61–70.

Patterson, J., Fenton, W.H., Thorstensen, J.R., Harvey, D.A., Skillman, D.R., Fried, R.E., Monard, B., O'Donoghue, D., Beshore, E., Martin, B., et al., 2002. Superhumps in cataclysmic binaries. XXIII. V442 ophiuchi and RX J1643. 7+ 3402. Publ. Astron. Soc. Pac. 114 (802), 1364. http://dx.doi.org/10.1086/344587.

Qian, S., Han, Z., Lajús, E.F., Zhu, L., Li, L., Liao, W., Zhao, E., 2015. Long-term decrease and cyclic variation in the orbital period of the eclipsing dwarf nova V2051 OPH. Astrophys. J. Suppl. 221 (1), 17. http://dx.doi.org/10.1088/0067-0049/221/1/17.

Ramsay, G., Cannizzo, J.K., Howell, S.B., Wood, M.A., Still, M., Barclay, T., Smale, A., 2012. Kepler observations of V447 Lyr: an eclipsing U gem cataclysmic variable. Mon. Not. R. Astron. Soc. 425 (2), 1479–1485. http://dx.doi.org/10.1111/j.1365-2966.2012.21657.x.

Ramsay, G., Wood, M.A., Cannizzo, J.K., Howell, S.B., Smale, A., 2017. V729 Sgr: a long period dwarf nova showing negative superhumps during quiescence. Mon. Not. R. Astron. Soc. 469 (1), 950–955. http://dx.doi.org/10.1093/mnras/stx859.

Scaringi, S., Groot, P., Still, M., 2013. Kepler observations of the eclipsing cataclysmic variable KIS J192748. 53+ 444724.5. MNRAS: Lett. 435 (1), L68–L72. http://dx.doi.org/10.1093/mnrasl/slt099.

Scepi, N., Begelman, M.C., Dexter, J., 2021. QPOs in compact binaries from small-scale eruptions in an inner magnetized disc. Mon. Not. R. Astron. Soc. 500 (1), 1547–1556. http://dx.doi.org/10.1093/mnras/staa3410.

Semeniuk, I., Olech, A., Kwast, T., Nalezyty, M., 1997. CCD photometry of SW ursae majoris during the 1996 superoutburst. http://dx.doi.org/10.1093/pasj/50.2.297, arxiv preprint arxiv:astro-ph/9704215.

Tovmasian, G., 1987. Quasiperiodic light variations of dwarf nova SS aurigae at quiescence. Astrofizika 27, 231–236.

Tremko, J., Andronov, I., Chinarova, L., Kumsiashvili, M., Luthardt, R., Pajdosz, G., Patkos, L., Roessiger, S., Zola, S., 1996. Periodic and aperiodic variations in TT arietis. Results from an international campaign. Astron. Astrophys. 312, 121–134.

Vogt, N., 1982. Z Chamaeleontis-evidence for an eccentric disk during supermaximum. Astrophys. J. 252, 653–667. http://dx.doi.org/10.1086/159592.

Warner, B., 1995. Cataclysmic Variable Stars, Vol. 28. Cambridge University Press.

Warner, B., 2004. Rapid oscillations in cataclysmic variables. Publ. Astron. Soc. Pac. 116 (816), 115. http://dx.doi.org/10.1086/381742.

Warner, B., Woudt, P.A., 2002. Dwarf nova oscillations and quasi-periodic oscillations in cataclysmic variables–II. A low-inertia magnetic accretor model. Mon. Not. R. Astron. Soc. 335 (1), 84–98. http://dx.doi.org/10.1046/j.1365-8711.2002.05596.x.

Warner, B., Woudt, P.A., Pretorius, M.L., 2003. Dwarf nova oscillations and quasi-periodic oscillations in cataclysmic variables–III. A new kind of dwarf nova oscillation, and further examples of the similarities to X-ray binaries. Mon. Not. R. Astron. Soc. 344 (4), 1193–1209. http://dx.doi.org/10.1046/j.1365-8711.2003.06905.x.

Wood, J., Irwin, M., Pringle, J., 1985. A digital technique for the separation of the eclipses of a white dwarf and an accretion disc. Mon. Not. R. Astron. Soc. 214 (4), 475–479. http://dx.doi.org/10.1093/mnras/214.4.475.

Wood, M.A., Still, M.D., Howell, S.B., Cannizzo, J.K., Smale, A.P., 2011. V344 lyrae: A touchstone su UMa cataclysmic variable in the Kepler field. Astrophys. J. 741 (2), 105. http://dx.doi.org/10.1088/0004-637X/741/2/105.

Woudt, P.A., Warner, B., 2002. Dwarf nova oscillations and quasi-periodic oscillations in cataclysmic variables–I. Observations of VW Hyi. Mon. Not. R. Astron. Soc. 333 (2), 411–422. http://dx.doi.org/10.1046/j.1365-8711.2002.05415.x.

Woudt, P.A., Warner, B., 2003. High-speed photometry of faint cataclysmic variables—III. V842 Cen, BY cir, DD cir, TV Crv, V655 CrA, CP Cru, V794 Oph, V992 Sco, EU Sct and V373 sct. Mon. Not. R. Astron. Soc. 340 (3), 1011–1019. http://dx.doi.org/10.1046/j.1365-8711.2003.06367.x.